

Lithospheric SH wave velocity structure beneath the northeastern Tibetan plateau from Love wave tomography

Yuanyuan V. Fu¹ Yuan Gao¹ and Lun Li²

¹Institute of Earthquake Forecasting, China Earthquake Administration, Beijing China

²School of Earth Sciences and Engineering, Sun Yat-sen University, Guangzhou, China

Introduction

The Cenozoic collision between the Indian and Eurasian plates has resulted in the formation of the Tibetan plateau in current stage. The modern plateau is characterized by high elevation with flat-topped and steep-sided morphology. Convergence and deformation continue today, but the mechanisms responsible for the plateau's uplift remain under debate. Previous studies suggested that the high topography could result from either a highly thickened upper crust through brittle faulting and folding or ductile flow and inflation of the lower crust, or deep-seated thermal buoyancy due to the delamination or convective removal of tectonically thickened lithospheric mantle. The question of whether upper crustal thickening, the crustal flow or mantle lithosphere dynamic process is responsible for the height in northeast (NE) Tibetan plateau remains obscure. The isotropic assumption and do not consider the effect of anisotropy. Given above mentioned ongoing debates, in this study we construct a high-resolution SH wave velocity (VSH) model from Love wave tomography based on the dense seismic array ChinArray II and the permanent China Digital Seismic Array in the NE Tibetan plateau (Figure 1). Our current high-resolution VSH model could provide more details and could offer a line of additional independent evidence on the existing controversies.

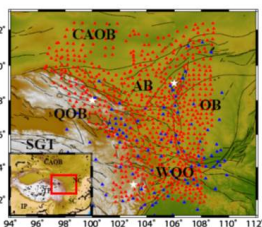


Fig. 1 Tectonic map of the northeastern Tibetan plateau. Red and blue triangles represent the temporary stations from ChinArray II and permanent stations from China Digital Seismic Array, respectively. White stars are the locations for the examples in Figure 7. IP, Indian Plate; TP, Tibetan Plateau; SC, South China; NC, North China; CAOB, Central Asian Orogenic Belt; AB, Alba Block; OB, Ordos Block; QOB, Qilian Orogenic Belt; SGT, Songpan-Ganzi Terrane; WQO, Western Qinling Orogen.

Methods

Phase velocity inversion

• Earthquake two-plane-wave tomography for the periods of 20-100 s (Li and Li, 2015)

Shear wave velocity inversion

• Invert shear wave velocity from Love wave phase velocities using the method of Saito (1988)

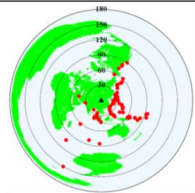


Fig. 2 Distribution of the teleseismic events (red circles) used in this study. The black triangle indicates the center of the seismic array.

Data

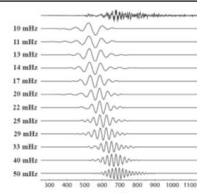


Fig. 3 An example of the waveforms of the fundamental-mode Love wave at station 64052 from an intermediate depth earthquake (24.2N, 122.3E) on April 20, 2015.

Resolution tests

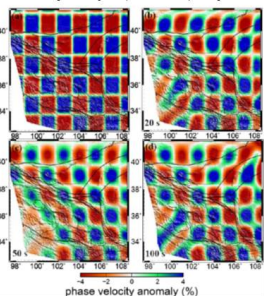


Fig. 4 Examples of checkerboard resolution tests. (a) Synthetic checkerboard model. The magnitudes of the input anomalies are 4% and sizes of anomalies are ~1.5°x1.5°. (b-d) Retrieved phase velocity at periods 20 s, 50 s and 100 s.

Phase velocity of Love wave

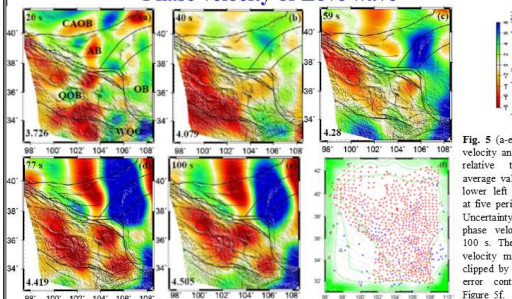


Fig. 5 (a-c) Phase velocity anomalies relative to the average value (the lower left corner) at five periods. (d-f) Uncertainty of the phase velocity at 100 s. The phase velocity maps are clipped by the 2% error contour in Figure 5f.

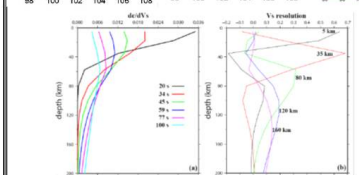


Fig. 6 (a) Phase velocity sensitivity kernel at six periods based on the AKI3.5 model. (b) Depth resolution of shear wave velocity from the model resolution matrix.

shear wave velocity

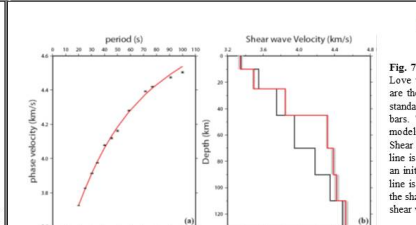


Fig. 7 (a) Observed and predicted average Love wave phase velocities. The triangles are the observed dispersion data with two standard deviations indicated by the error bars. The predicted from the best fitting models in (b) are shown as red line. (b) Shear wave velocity models. The black line is the modified AKI3.5 model used as an initial model for the inversion. The red line is the best fitting model. The width of the shaded area shows the standard error of shear wave velocity in each layer.

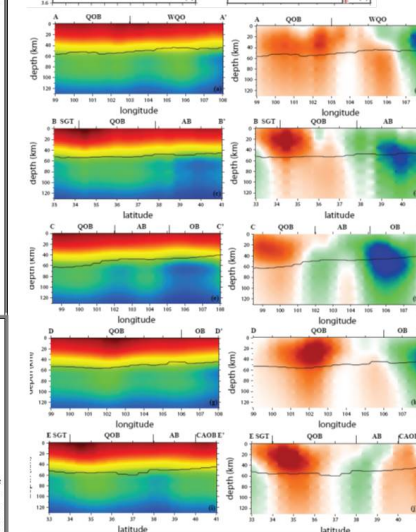


Fig. 9 Vertical slices of the absolute shear wave velocity (a, c, e, g and i) and velocity anomaly (b, d, f, h and j) along five profiles with locations shown in Figure 8a.

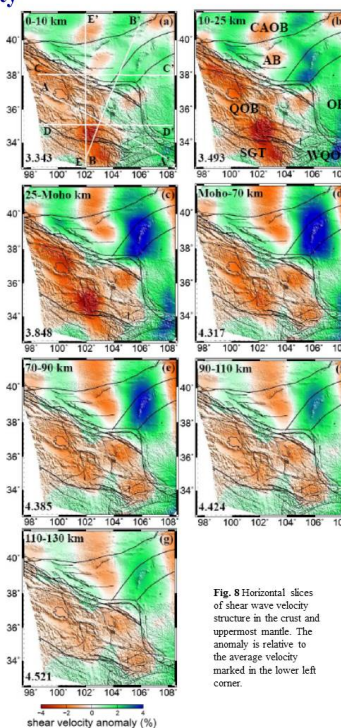


Fig. 8 Horizontal slices of shear wave velocity structure in the crust and uppermost mantle. The anomaly is relative to the average velocity marked in the lower left corner.

Summary

- Widespread zones of low wave speed at mid-lower crustal depth is observed beneath the NE Tibetan plateau. The reduced shear wave speed could be attributed to partial melt in the crust.
- Slow SH wave velocity is also observed in the uppermost mantle of northeast Tibetan plateau, indicating a warm and weak lithosphere. This slow velocity could result from asthenosphere upwelling after lithospheric mantle removal in the NE Tibetan plateau. The consequence of the asthenosphere upwelling is the occurrence of partial melting in the mid-lower crust and a portion of high topography in this region via deep-seated thermal buoyancy after delamination.
- Fast SH wave velocity appears in the western Qinling orogen from the surface to the depth of 130 km, implying that the lower crustal channel flow model probably does not work in this region.